Ramiro Pérez Campos
Antonio Contreras Cuevas
Rodrigo A. Esparza Muñoz *Editors*

Characterization of Metals and Alloys

Springer

Characterization of Metals and Alloys

Ramiro Pérez Campos • Antonio Contreras Cuevas
Rodrigo A. Esparza Muñoz
Editors

Characterization of Metals and Alloys

Springer

Editors
Ramiro Pérez Campos
Centro de Física Aplicada y
Tecnología Avanzada (CFATA)
Querétaro, México

Antonio Contreras Cuevas
Instituto Mexicano del Petróleo
Distrito Federal
México

Rodrigo A. Esparza Muñoz
Centro de Física Aplicada y
Tecnología Avanzada (CFATA)
Querétaro, México

ISBN 978-3-319-31693-2 ISBN 978-3-319-31694-9 (eBook)
DOI 10.1007/978-3-319-31694-9

Library of Congress Control Number: 2016952548

Printed on acid-free paper

This Springer imprint is published by Springer Nature
The registered company is Springer International Publishing AG Switzerland

Chapter 15
Microwave Assisted Sol-Gel Synthesis and Characterization of M–TiO_2 (M=Pt, Au) Photocatalysts

R. Hernández, S.M. Durón-Torres, K. Esquivel, and C. Guzmán

Abstract Pt–TiO_2 and Au–TiO_2 photocatalysts have been synthetized by a microwave assisted sol-gel method and characterized by means of X-ray diffraction (XRD) techniques and UV-Vis diffuse reflectance spectroscopy. Particle sizes have been determined by means of Scherrer equation. Depending on the weight percentage of dopant, some changes in the band gap energy can be observed. X-ray diffractions patterns were recorded to study the formation of TiO_2 crystalline species. The diffraction peaks detected after the calcination process indicate the presence of the crystalline anatase phase and no presence of rutile phase was observed. For the Pt–TiO_2 sample, the peaks detected in 2θ (39.4°, 45.9°, and 67°) indicate the presence of particles of metallic platinum. For the Au–TiO_2 sample, the peaks detected in 2θ (38°, 44.2°, 64.4°, and 77.2°) indicate the presence of particles of metallic gold. The Pt-loaded samples have a crystal size slightly smaller than the Au-loaded samples, from 3.09 to 4.74 nm. UV-Vis DSR technique was used to study the influence of metal load and type. The band gap decreases according to the metal load; it shows that at higher metal load (5 %) the band gap changes from 3.2 eV (pure TiO_2) to 2.98 eV and 3.04 eV for the samples loaded with gold and platinum, respectively. For the Pt–TiO_2 sample, the band gap varies from 3.04 eV (5 wt.%) to 3.2 eV (0.1 wt.%), the same behavior is found on the Au-loaded samples, with a band gap energy variation from 2.98 eV (5 wt.%) to 3.21 eV (0.01 wt.%).

Keywords Titanium dioxide • Photocatalysis • Pt-TiO_2 • Au-TiO_2 • X-ray diffraction

R. Hernández • S.M. Durón-Torres • C. Guzmán (✉)
UACQ—UAZ, CU Siglo XXI Edificio 6, Km 6 Carr. Zac – Gdl, La Escondida Zacatecas, Zac C.P. 96160, Mexico
e-mail: rafita_bot@hotmail.com; cgm1909@hotmail.com; cguzman@uaq.mx

K. Esquivel
Facultad de Ingeniería, Universidad Autónoma de Querétaro, Cerro de las Campanas, C.P. 76000 Santiago de Querétaro, Queretaro, Mexico

R. Pérez Campos et al. (eds.), *Characterization of Metals and Alloys*, DOI 10.1007/978-3-319-31694-9_15

15.1 Introduction

Titanium dioxide (TiO_2) has been widely used and investigated due to the stability of its chemical structure, biocompatibility, and its physical, optic, and electric properties. Its photocatalytic properties have been utilized in many environmental applications to remove pollutants in water and air. The main feature of the photocatalytic process is that it breaks the complex organic molecules into simple molecules such as carbon dioxide and water; this process has been used for a variety of applications such as decomposition of organic pollutants [1].

TiO_2 exists as three different polymorphs: anatase, rutile, and brookite. The most stable form of TiO_2 is rutile. Anatase form has a crystalline structure corresponding to a tetragonal system and is used mostly in photocatalytic applications due to its photocatalytic activity under UV radiation. Rutile form of TiO_2 has a tetragonal structure and brookite an orthorhombic structure [2].

Typically, titanium dioxide is an n-type semiconductor. The energy gap is 3.2 eV for anatase, 3.0 eV for rutile, and 3.2 eV for brookite. Generally, anatase form of TiO_2 is desired owing to its higher photo activity, high superficial area, and low toxicity. Due to its high photoinduced reduction, anatase form is a better photocatalytic material for degradation of organic pollutants in both water and air [3].

The application of TiO_2 is limited due to its low photoactivity under visible light. Therefore, attempts to extend its photoactivity to the visible region have been made by substitution of Ti^{4+} on the crystalline structure for metallic ions such as Fe, Ni, Co, Ag, Au, Pt, etc. [4–8].

Sol-gel synthesis technique has been widely used for catalysts development, such as TiO_2 nanopowders. In comparison to traditional techniques, it offers many advantages. For instance, in supported metals catalysis, the active metal and support can be prepared in a single step. This allows an economy in the catalyst preparation [9].

In the present paper, we report the synthesis and characterization of Pt–TiO_2 and Au–TiO_2 catalyst prepared by the microwave assisted sol-gel technique.

15.2 Experimental

The synthesis of the TiO_2 catalyst was carried out by dissolving the titanium precursor (titanium isopropoxide) in an organic solvent (isopropanol, 99.9 %), and the titanium solution was magnetically stirred for 20 min under nitrogen atmosphere. The hydrolysis process was then performed by adding water into the precursor/solvent solution and was magnetically stirred for 1 h in a dark box. For the Pt-modified TiO_2 samples, the platinum precursor was $H_2Pt(NO_2)_2SO_4$, and for the Au-modified TiO_2 samples, the precursor was $NaAuCl_4 \cdot 2H_2O$. These precursors were added by dissolving them into the water used for the hydrolysis

process in different weight percentage (0.01, 0.05, 0.1, 0.5, 1, and 5 wt.%). The obtained sol was transferred into Teflon vessels and placed on a microwave reaction system. The heating procedures were carried for 30 min at 220 °C. The obtained product was filtered and dried at room temperature for 12 h. A calcination process was carried out at 450 °C for 3 h to promote the anatase form of TiO_2.

15.2.1 Photocatalyst Characterization

Elemental analysis was performed by Energy Dispersive X-ray Spectroscopy (EDS) (EDS Oxford Inca X-Sight coupled to an MT 1000, Hitachi). Particle size was determined using Scherrer equation [10]. Band gap energy (Ebg) values were determined from diffuse reflectance measurements (Cary 5000 UV-Vis-NIR Varian spectrophotometer) by applying Kubelka–Munk [11] function and Tauc's graphics.

15.3 Results and Discussion

15.3.1 X-ray Diffraction

X-ray diffractions (XRDs) patterns were recorded to study the formation of TiO_2 crystalline species. The diffraction peaks detected after the calcination process indicate the presence of the crystalline anatase phase and no presence of rutile phase was observed. For the Pt–TiO_2 samples (Fig. 15.1a), the peaks detected in 2θ (39.4°, 45.9°, and 67°) indicate the presence of particles of metallic platinum. For the Au–TiO_2 samples (Fig. 15.1b), the peaks detected in 2θ (38°, 44.2°, 64.4°, and 77.2°) indicate the presence of particles of metallic gold. As can be seen from the XRD patterns crystallinity of the photocatalyst decreased on platinum and gold doping.

The crystallite sizes were calculated by the Scherrer equation and are compiled in Table 15.1. The Au-loaded samples have a crystallite size between 4.74 nm for 5 wt.% of gold and 3.17 nm for 0.05 wt.% of gold. The Pt-loaded samples have sizes between 3.17 and 10.7 nm for 5 and 0.1 wt.% of platinum, respectively.

15.3.2 Raman Spectroscopy

Another technique widely used to characterize various polymorphs of TiO_2 is Raman spectroscopy. Some advantages of using this technique are the sample preparation and the simplicity with which each spectrum is collected [12].

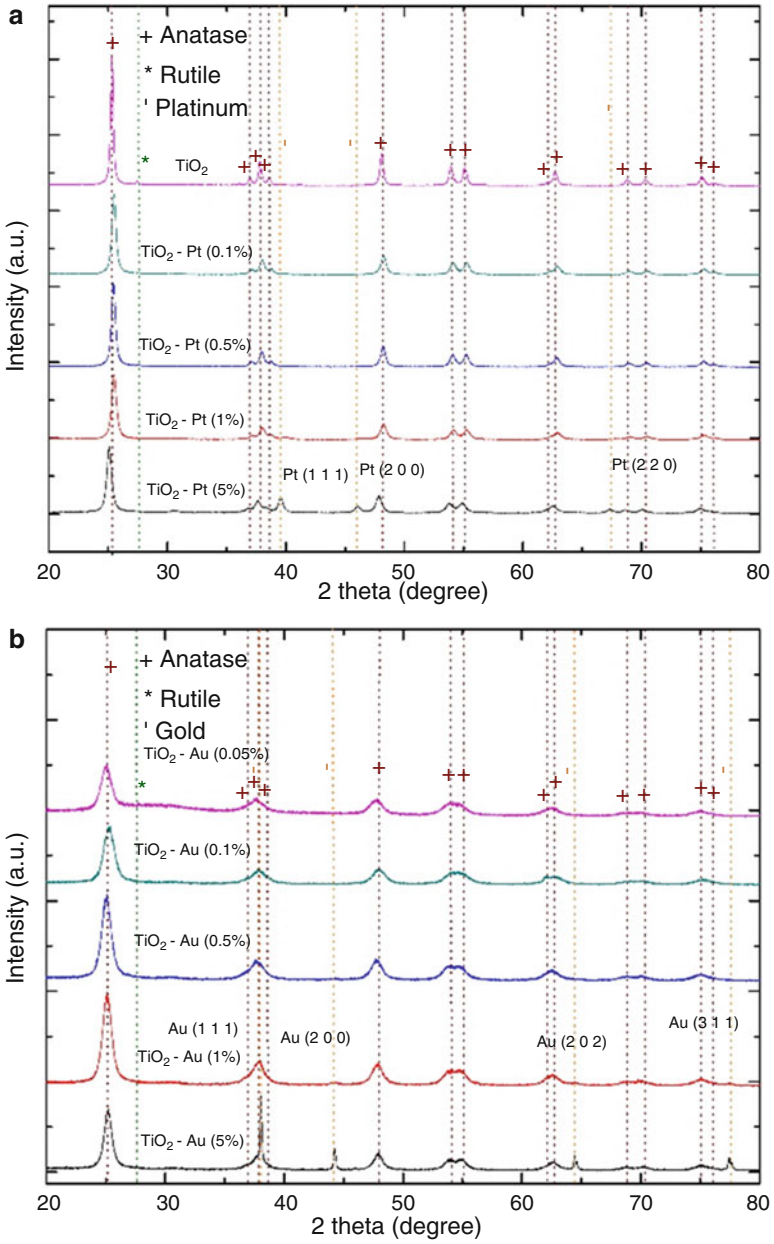

Fig. 15.1 XRD diffraction patterns of synthetized TiO_2, (**a**) Pt-TiO_2 and (**b**) Au-TiO_2

Table 15.1 Crystallite sizes

Photocatalyst	Crystallite sizes (nm)	Crystallite sizes (nm)	Photocatalyst
TiO_2–Au (5 %)	4.74	3.71	TiO_2–Pt (5 %)
TiO_2–Au (1 %)	4.10	11.2	TiO_2–Pt (1 %)
TiO_2–Au (0.5 %)	3.97	10.8	TiO_2–Pt (0.5 %)
TiO_2–Au (0.1 %)	3.59	10.7	TiO_2–Pt (0.1 %)
TiO_2–Au (0.05 %)	3.17	–	–

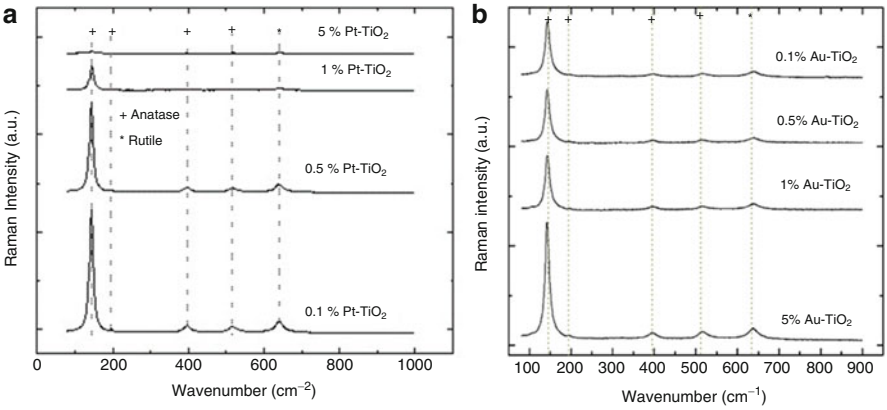

Fig. 15.2 Raman spectroscopy patterns of synthetized TiO_2, (**a**) Pt-TiO_2 and (**b**) Au-TiO_2

For anatase, characteristic vibration modes are located at 144, 197, 399, 515, and 639 cm^{-1}. For rutile, there are four modes at 143, 235, 447, and 612 and a broadband at 826 cm^{-1}. Brookite has 36 vibration modes, some of them located at 132, 138, 152, 197, 212, 245, 278, 325, 370, 406, 457, 500, 550, 587, and 630 cm^{-1}. The most intense vibration mode for anatase is at 144 cm^{-1}, and the weakest for rutile is at 143 cm^{-1} [13].

Figure 15.2 shows the Raman spectra for samples synthetized at different dopant loads. In order to make identification of the vibration modes easer, the spectra were arbitrarily displaced on the vertical axis. Pt-loaded samples show a spectrum with well-defined vibration modes assigned to anatase (144, 197, 399, and 515 cm^{-1}) and rutile (612 cm^{-1}). Au-loaded samples show a spectrum with well-defined vibration modes assigned to anatase (144, 197, 399, 515, and 639 cm^{-1}) and no characteristic vibration modes of rutile or brookite were observed.

15.3.3 Band Gap Measurements

UV-Vis DSR technique was used to study the influence of metal load and type. The Tauc's graphics showed in Fig. 15.3a, b for Pt–TiO_2 and Au–TiO_2, respectively, are utilized to estimate the band gap energies by means of Kubelka–Munk method.

The band gap energies estimated are listed in Table 15.2. The band gap decreases according to the metal load; it shows that at higher metal load (5 %) the band gap changes from 3.2 eV (pure TiO_2) to 2.98 eV and 3.04 eV for the samples loaded with gold and platinum, respectively.

For the Pt–TiO_2 sample, the band gap varies from 3.04 eV (5 wt.%) to 3.2 eV (0.1 wt.%), the same behavior is found on the Au-loaded samples, with a band gap energy variation from 2.98 eV (5 wt.%) to 3.21 eV (0.01 wt.%). It is interesting to note that the band gap energies increase on metal doping for both platinum and gold.

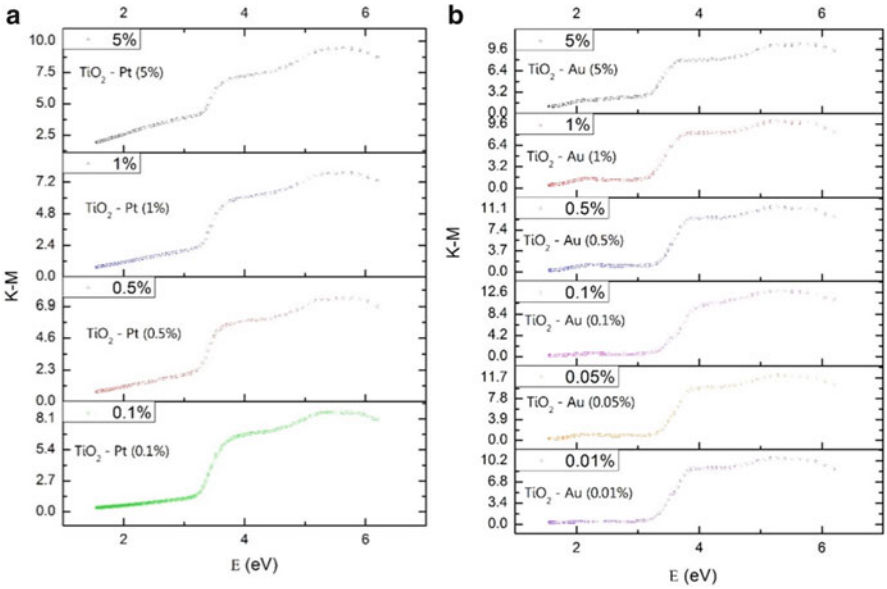

Fig. 15.3 Raman spectroscopy patterns of synthetized TiO_2, (**a**) Pt-TiO_2 and (**b**) Au-TiO_2

Table 15.2 Band gap energies

Photocatalyst	Band gap (eV)	Band gap (eV)	Photocatalyst
TiO_2–Au (5 %)	2.98	2.87	TiO_2–Pt (5 %)
TiO_2–Au (1 %)	3.05	3.09	TiO_2–Pt (1 %)
TiO_2–Au (0.5 %)	3.23	3.05	TiO_2–Pt (0.5 %)
TiO_2–Au (0.1 %)	3.24	3.15	TiO_2–Pt (0.1 %)
TiO_2–Au (0.05 %)	3.19	–	–

15.4 Conclusions

Microwave assisted synthesis methodology can be applied for the preparation of TiO_2-based photocatalysts and modify its properties using a dopant metal such as Au and Pt. With these metals it is possible to observe a change in the band gap energy, which can be related to the metal load in the photocatalyst.

References

1. Macwan DP, Dave PN, Chaturvedi S (2011) A review on nano-TiO2 sol–gel type syntheses and its applications. J Mater Sci 11:3669–3686
2. Pelaez M, Nolan NT, Pillai SC, Seery MK, Falaras P, Kontos AG, Dunlop PSM, Hamilton JWJ, Byrne JA, O'Shea K, Entezari MH, Dionysiou DD (2012) A review on the visible light active titanium dioxide photocatalysts for environmental applications. Appl Catal B Environ 125:331–349
3. Esquivel K, Nava R, Zamudio-Méndez A, González MV, Jaime-Acuña OE, Escobar-Alarcón L, Peralta-Hernández JM, Pawelec B, Fierro JLG (2013) Microwave-assisted synthesis of (S)Fe/TiO2 systems: effects of synthesis conditions and dopant concentration on photoactivity. Appl Catal B Environ 140:213–224
4. Khan AW, Ahmad S, Mehedi Hassan M, Naqvi AH (2014) Structural phase analysis, band gap tuning and fluorescence properties of Co doped TiO2 nanoparticles. Opt Mater 38:278–285
5. Kobayashi Y, Ishii Y, Yamane H, Watanabe K, Koda H, Kunigami H, Kunigami H (2014) Fabrication of TiO2/Pt core–shell particles by electroless metal plating. Colloids Surf Physicochem Eng Asp 448:88–92
6. Lei XF, Xue XX, Yang H (2014) Preparation and characterization of Ag-doped TiO2 nanomaterials and their photocatalytic reduction of Cr(VI) under visible light. Appl Surf Sci 321:396–403
7. Liu Q, Ding D, Ning C, Wang X (2015) Black Ni-doped TiO2 photoanodes for high-efficiency photoelectrochemical water-splitting. Int J Hydrog Energy 40:2107–2114
8. Park H, Park Y, Kim W, Choi W (2013) Surface modification of TiO2 photocatalyst for environmental applications. J Photochem Photobiol Photochem Rev 15:1–20
9. Sánchez E, López T, Gómez R, Bokhimi, Morales A, Novaro O (1996) Synthesis and characterization of sol–gel Pt/TiO2, catalyst. J Solid State Chem 122:309–314
10. Patterson AL (1939) The Scherrer formula for X-ray particle size determination. Phys Rev 56:978–982
11. Escobedo Morales A, Sánchez Mora E, Pal U (2007) Use of diffuse reflectance spectroscopy for optical characterization of un-supported nanostructures. Rev Mex Fis Suppl 53:18–22
12. Leyva-Porras C, Toxqui-Teran A, Vega-Becerra O, Miki-Yoshida M, Rojas-Villalobos M, García-Guadarrama M, Aguilar-Martinez JA (2015) Low-temperature synthesis and characterization of anatase TiO2 nanoparticles by an acid assisted sol–gel method. J Alloys Compd 647:627–636
13. Zhang J, Li M, Feng Z, Chen J, Li C (2006) UV raman spectroscopic study on TiO2. Phase transformation at the surface and in the bulk. J Phys Chem B 110:927–935